A Highly-Accurate Finite Element Method with Exponentially Compressed Meshes for the Solution of the Dirichlet Problem of the generalized Helmholtz Equation with Corner Singularities

Celiker, Emine; Lin, Ping

Published in:
Journal of Computational and Applied Mathematics

DOI:
10.1016/j.cam.2019.04.004

Publication date:
2019

A Highly-Accurate Finite Element Method with Exponentially Compressed Meshes for the Solution of the Dirichlet Problem of the generalized Helmholtz Equation with Corner Singularities

Emine Celiker*[1] and Ping Lin†[1]

[1]Division of Mathematics, University of Dundee, 23 Perth Road, Dundee, Scotland, DD1 4HN, UK

Abstract

In this study, a highly-accurate, conforming finite element method is developed and justified for the solution of the Dirichlet problem of the generalized Helmholtz equation on domains with re-entrant corners. The $k-th$ order Lagrange elements are used for the discretization of the variational form of the problem on exponentially compressed polar meshes employed in the neighbourhood of the corners whose interior angle is $\alpha\pi$, $\alpha \neq 1/2$, and on the triangular and curved mesh formed in the remainder of the polygon. The exponentially compressed polar meshes are constructed such that they are transformed to square meshes using the Log-Polar transformation, simplifying the realization of the method significantly. For the error bound between the exact and the approximate solution obtained by the proposed method, an accuracy of $O(h^k)$, h mesh size and $k \geq 1$ an integer, is obtained in the H^1-norm. Numerical experiments are conducted to support the theoretical analysis made. The proposed method can be applied for dealing with the corner singularities of general nonlinear parabolic partial differential equations with semi-implicit time discretization.

Keywords: mesh refinement, Helmholtz equation, singularity problem, finite element method, error analysis.

MSC 2010. 65N30, 65N50, 65N15, 65N12, 65N22.

1 Introduction

Singularities are often encountered in the solution of elliptic equations in two dimensions due to the non-smoothness of the boundary of the domain and the abrupt changes of the boundary conditions. The classical finite-difference and finite-element methods become ineffective around the singular points, and hence various methods with special constructions have been proposed in order to obtain approximate solutions with the required order of accuracy.

To name a few of these methods, Babuška and Oh [1], Thatcher [2] and Burda et. al. [3] used mesh refinement in the neighbourhood of the singular points; Fix [4], and Wait and Mitchell [5]

*Corresponding Author: eceliker@dundee.ac.uk; Tel: 01382 384485

†plin@dundee.ac.uk, Tel: 01382 384473, Fax: 01382 385516

applied a finite element method using bilinear basis functions supplemented by singular functions; Li [6] used a nonconforming combined method and Dosiyev [7] combined the finite-difference method with the integral representation of the solution; Wu and Han [8] dealt with the problem by introducing an artificial boundary and using the finite-element method in the domain away from the singularities. Furthemore, Xenophontos et. al. [9] applied a singular function boundary integral method, Volkov [10] used a method based on the integral representation of the solution, and Magura et. al. [11] employed the method of difference potentials to obtain a solution with high-order accuracy.

Even though these methods successfully provide approximate solutions of required accuracy, the implementation becomes much more challenging. For instance, using singular basis functions as part of a combined method leads to the loss of sparsity of the coefficient matrix ([5], [12]). Moreover, most of the studies constructing methods based on mesh refinement techniques employ algebraically refined meshes ([1]-[3], [13], [14]), which can lead to a deterioration of conditioning since the mesh is refined very aggressively near the singularity to maintain high-order accuracy.

In this paper, we propose an efficient, highly accurate finite-element method for the solution of the generalized Helmholtz equation on polygons, based on the *a priori* estimates of the solution. The Helmholtz equation, which is the time-independent form of the wave equation, arises in real life applications such as the scattering of radar waves near an air-ocean-sea interface [15].

In order to overcome the reduction in the accuracy of the approximate solution caused by corner singularities, exponentially refined polar meshes are constructed near the corners of the solution domain. The uniform mesh in the remainder of the domain is conforming with the polar meshes so that no additional techniques are required for coupling the solution in the subdomains.

The proposed local mesh refinement is exponential in the polar radius r and uniform in the polar angle θ. A similar technique of mesh refinement was introduced by E. A. Volkov in [16] as part of a composite grids method for a second-order accurate solution on polygons, where an overlapping domain-decomposition method was constructed with exponentially compressed polar meshes in the neighbourhood of the corners, coupled with square grids in the overlapping rectangles covering the remainder of the domain. The finite-difference method was applied for the approximate solution. Fourth and sixth order accurate composite grids methods were developed by E. A. Volkov and A. A. Dosiyev in [17] and [18] respectively. However, the composite grids method is only justified for the solution of the boundary value problem of Laplace's equation, and highly accurate solutions are restricted to staircase polygons.

For the implementation of the proposed method, the exponentially compressed meshes are transformed to square meshes in Log-Polar coordinates, hence there is no need to design a special mesh or to derive a new algorithm for the solution in the neighbourhood of the corners. The use of exponentially compressed meshes also has the advantage of much faster refinement compared to algebraically refined meshes, leading to a finite-element system with smaller number of equations.

For the error bound between the exact and the approximate solution obtained by the proposed method, an accuracy of $O(h^k)$, where h is the maximum mesh size and $k \geq 1$ is an integer, is obtained in the H^1-norm. Numerical experiments are conducted to support the theoretical analysis made, and to demonstrate the efficiency of the implementation of the method. The numerical results are consistent with the theoretical results obtained.

The structure of the paper is as follows. In Section 2 we give the problem formulation and discuss the asymptotic expansion of the solution in the vicinity of corners. In Section 3 we describe the proposed method for computing the highly-accurate approximate solution of the generalized Helmholtz equation with Dirichlet boundary conditions on polygons. Section 4 is devoted to the error analysis of the method. In Section 5 we present the solutions of a numerical example solved by the proposed method, and finally concluding remarks are given in Section 6.

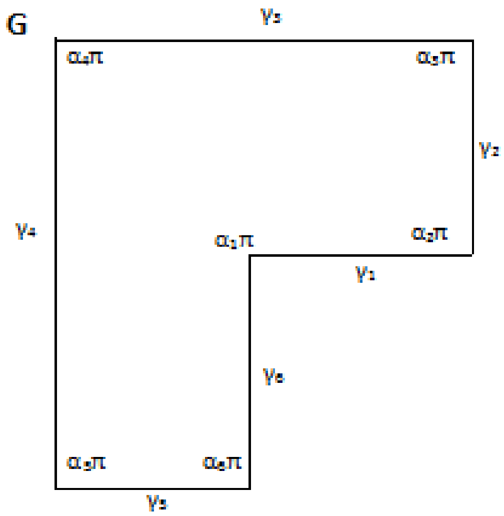

Figure 1: A polygonal domain described in Section 2

2 Problem Statement

Let G be an open simply-connected polygon , γ_j, $j = 1, ..., N$, be its sides, including the ends, enumerated counter-clockwise, let $\gamma = \cup_{j=1}^{N} \gamma_j$ be the boundary of G, $\overline{G} = G \cup \gamma$, and $\alpha_j \pi$, $0 < \alpha_j \leq 2$, be the interior angle formed by the sides γ_{j-1} and γ_j ($\gamma_0 \equiv \gamma_N$) (see Figure 1). Further we denote by $A_j = \gamma_{j-1} \cap \gamma_j$ the $j - th$ vertex of G and by r_j, θ_j a polar system of coordinates with pole in A_j and the angle θ_j taken counter-clockwise from the side γ_j.

Consider the boundary value problem

$$-\Delta u + a_0 u = f \text{ on } G, \tag{1}$$

$$u = \phi_j \text{ on } \gamma_j, \tag{2}$$

where $\Delta \equiv \frac{\partial^2}{\partial x^2} + \frac{\partial^2}{\partial y^2}$, $a_0 > 0$ is a constant and f, ϕ_j, $j = 1, ..., N$, are given functions.

We assume that

$$f \in H^{k-1}(G), \ \phi_j \in H^{k+1}(\gamma_j), \ j = 1, 2, ...N, \tag{3}$$

where $H^k(S)$ denotes the Sobolev space equipped with the norms and seminorms

$$||v||_{k,S} = \left(\sum_{|\alpha| \leq k} \iint_S |D^\alpha v|^2 dS \right)^{1/2},$$

$$|v|_{k,S} = \left(\sum_{|\alpha| = k} \iint_S |D^\alpha v|^2 dS \right)^{1/2},$$

respectively.

Problem (1), (2) is formulated in weak form as follows:
Find $u \in H^1_E(G)$ such that $u|_{\gamma_j} = \phi_j$ and

$$a(u,v) = (f,v), \tag{4}$$

$\forall v \in H^1_0(G)$, where

$$a(u,v) = \iint_G \left(\frac{\partial u}{\partial x}\frac{\partial v}{\partial x} + \frac{\partial u}{\partial y}\frac{\partial v}{\partial y} + a_0 uv \right) dxdy, \tag{5}$$

$$(f,v) = \iint_G fv\ dxdy, \tag{6}$$

$$H^1_E(G) = \left\{ v | v, \frac{\partial v}{\partial x}, \frac{\partial v}{\partial y} \in L^2(G) \text{ and } v|_{\gamma_j} = \phi_j, j = 1,2,...,N \right\}$$

and

$$H^1_0(G) = \left\{ v | v, \frac{\partial v}{\partial x}, \frac{\partial v}{\partial y} \in L^2(G) \text{ and } v|_{\gamma} = 0 \right\}.$$

In the vicinity of each vertex A_j of the polygon G, the exact solution of the boundary value problem (1), (2) can be represented as an asymptotic expansion. Specifically, consider the boundary value problem

$$-\Delta u + a_0 u = f \text{ on } S_j, \tag{7}$$
$$u|_{\gamma_{j-1}} = \phi_{j-1},\ u|_{\gamma_j} = \phi_j, \tag{8}$$

where S_j is a wedge in the neighbourhood of A_j whose boundary coincides with γ_{j-1} and γ_j.
The solution is written in the form

$$u = u_H + u_P, \tag{9}$$

where u_H is the solution to the homogeneous problem corresponding to (7), (8), and u_P is the particular solution.

We assume that the function $u_1(r_j, \theta_j)$ satisfies the boundary value problem

$$-\Delta u_1 + a_0 u_1 = 0 \text{ on } S_j, \tag{10}$$
$$u_1|_{\gamma_{j-1}} = \phi_{j-1},\ u_1|_{\gamma_j} = \phi_j. \tag{11}$$

and use a transformation $u_2 = u_H - u_1$ to lead to homogeneous boundary conditions.

It is well known that the function $u_2(r_j, \theta_j)$, which satisfies equation (10) and $u_2|_{\gamma_{j-1}} = u_2|_{\gamma_j} = 0$ has the form

$$u_2(r_j, \theta_j) = \sum_{n=1}^{\infty} b_n I_{n/\alpha_j}(a_0 r_j) \sin\left(\frac{n\theta_j}{\alpha_j}\right), \tag{12}$$

where the coefficients b_n are determined by the boundary data on the outer arc connecting the two rays forming the wedge and

$$I_{n/\alpha_j}(a_0 r_j) = \left(\frac{a_0 r_j}{2}\right)^{n/\alpha_j} \sum_{i=1}^{\infty} \frac{(a_0 r_j)^{2i}}{4^i i! \Gamma(i+1+n/\alpha_j)}$$

is the modified Bessel function of the first kind of order n/α_j. An asymptotic series for the function u_1 that satisfies problem (10), (11) can also be expressed as

$$u_1(r_j,\theta_j) = \sum_{m=1}^{\infty} r_j^m \left(A_m(\theta_j)\ln r_j + B_m(\theta_j)\right). \tag{13}$$

The particular solution u_P is the solution of the following boundary value problem:

$$-\Delta u_P + a_0 u_P = f \text{ on } S_j, \tag{14}$$
$$u_P|_{\gamma_{j-1}} = 0,\ u_P|_{\gamma_j} = 0. \tag{15}$$

For the series solution of problem (14), (15), the function f is expanded in the form

$$f = \sum_{i=1}^{\infty} f_i(\theta_j) r_j^i.$$

With the use of the eigenfunction expansion of Green's function, the solution of problem (14), (15) can be written as

$$u_P(r_j,\theta_j) = -\frac{2}{\alpha_j\pi}\int_{S_j}\left(\sum_{n=1}^{\infty}\frac{\varphi_n(\theta_j)\varphi_n(\theta_0)}{(n/\alpha)^2}\right)\left(\sum_{i=1}^{\infty} f_i(\theta_0) r_0^i\right) d^2\mathbf{r}_0, \tag{16}$$

where $\varphi_n(\theta) = \sin(n\theta/\alpha_j)$ and $\mathbf{r}_0 = (r_0,\theta_0)$.

It can be easily observed that for $1 < \alpha_j \le 2$, $\partial u/\partial r_j \to \infty$ as $r_j \to 0$ (a strong singularity), and for $0 < \alpha_j \le 1$, even though the first-order derivatives are bounded, the second-order derivatives might not be (a weak singularity).

3 Description of the Method

Let E denote the set of j, $(1 \le j \le N)$, for which $\alpha_j \ne 1/2$, or $\alpha_j = 1/2$ and the boundary functions ϕ_{j-1} and ϕ_j are not compatible on A_j. In the neighbourhood of each vertex A_j, $j \in E$, we construct a fixed sector $T_j = T_j(r_{j0}) \subset G$, where

$$T_j(r_{j0}) = \{(r_j,\theta_j) : 0 < r_j < r_{j0}, 0 < \theta_j < \alpha_j\pi\},$$

$r_{j0} > 0$ denotes the radius of the sector, γ_{j-1} and γ_j are the sides of the sector T_j, which coincide with the boundary of G, and ϑ_{j0} denotes the arc of the circle with radius r_{j0} and centre A_j, which is the curvilinear part of the boundary of the sector T_j. Hence $\Gamma_j = \gamma_{j-1}\cup\gamma_j\cup\vartheta_{j0}$ denotes the boundary of T_j, $\overline{T}_j = \Gamma_j \cup T_j$, and $T_n \cap T_m = \emptyset$, $n,m \in E$. Let $G^* = G\backslash\left(\cup_{j\in E}T_j\right)$. We assume that

$$u \in H^{k+1}(G^*). \tag{17}$$

For the solution of problem (24) in G^*, a finite element mesh is formed using triangular and curved elements. The solution is based on $k-th$ order Lagrange elements, which are C^0-continuous, P_k finite elements.

The curved elements, denoted t_c, are employed in the layer of elements adjacent to the curve (r_{j0},θ_j), $0 \le \theta_j \le \alpha_j\pi$, $j \in E$, and are of the form described by Zlámal in [19]. The transformation introduced by Zlámal ([19]-[21]), namely

$$x = x^*(\xi,\eta) \equiv x_1 + (x_2-x_1)\xi + (x_3-x_1)\eta + (1-\xi-\eta)\Phi^*(\eta), \tag{18}$$
$$y = y^*(\xi,\eta) \equiv y_1 + (y_2-y_1)\xi + (y_3-y_1)\eta + (1-\xi-\eta)\Psi^*(\eta), \tag{19}$$

is used to map the unit triangle $\overline{\tau}_1$ with vertices $R_1(0,0)$, $R_2(1,0)$, $R_3(0,1)$ in the ξ,η-plane on the closed element t_c with the required order of accuracy, where (x_i,y_i), $i=1,2,3$, are coordinates of the vertex Q_i of t_c, and the functions Φ^*, Ψ^* are constructed with the use of $k-th$ order Lagrange polynomials approximating the parametric equations representing the curved side of t_c. As stated in [19], it will not be necessary to carry out the inversion $\xi=\xi(x,y)$, $\eta=\eta(x,y)$ in actual computations.

We introduce the parameter $h>0$, which denotes the largest side in any element of the mesh on G^* (in the case of a curved element this means the triangle with the same vertices), and let G_h^* denote the finite element mesh formed on G^*.

In each sector $\overline{T}_j$, $j\in E$, a polar mesh is constructed with the family of rays $\theta_{jp}=p\beta_j$, $p=0,1,...,\alpha_j\pi/\beta_j$, with maximum angular step

$$\beta_j \le \min\{\alpha_j\pi/6, h\}, \tag{20}$$

where γ_{j-1} and γ_j are situated on the extreme rays, and with the family of circles with centers at A_j and radii $r_{jq}=r_{j0}\exp(-q\beta_j)$, $q=0,1,...,\nu_j$,

$$\nu_j = 1+\left[\max\left\{k, \frac{(k+1/2)\ln h^{-1}}{\beta_j \min\{1,1/\alpha_j\}}\right\}+N_{j0}\right], \tag{21}$$

where $N_{j0}\ge 0$ is an arbitrary fixed number, and [.] indicates the integer part. Condition (20) ensures that the parameter h denotes the largest side in any element on the constructed mesh, and the choice of ν_j is justified in the error analysis presented in Chapter 4.

We denote by T_j^h the finite-element mesh constructed on T_j, with boundary $\tilde{\Gamma}_j=\bar{\gamma}_{j-1}\cup\bar{\gamma}_j\cup\vartheta_{j0}\cup\vartheta_{j\nu_j}$, where $\vartheta_{j\nu_j}$ is the arc of the circle with radius $r_{j\nu_j}$ and centre A_j lying inside T_j,

$$\bar{\gamma}_j = \{(r_j,\theta_j): r_{j\nu_j}\le r_j\le r_{j0}, \theta_j=0\},$$

$$\bar{\gamma}_{j-1} = \{(r_j,\theta_j): r_{j\nu_j}\le r_j\le r_{j0}, \theta_j=\alpha_j\pi\},$$

and $\overline{T}_j^h=T_j^h\cup\tilde{\Gamma}_j$.

On the artificial boundary $\vartheta_{j\nu_j}$, the Lagrange polynomial

$$\phi_j^*(\theta_j)=\frac{(\alpha_j\pi-\theta_j)\overline{\phi}_j+\theta_j\overline{\phi}_{j-1}}{\alpha_j\pi} \tag{22}$$

is applied as the boundary function, where $\overline{\phi}_\mu$, $\mu=j-1,j$, denotes the value of the boundary function ϕ_μ at a point on γ_μ, whose distance from the vertex A_j is $r_{j\nu_j}$. The mesh G_h^* is chosen to be conforming with each $\overline{T}_j^h$, so that no additional techniques are required for the connection of the subdomains.

The exponentially compressed grid constructed in $\overline{T}_j$, $j\in E$, is demonstrated in Figure 2 on a staircase polygon with one singular corner.

The approximate solution of the variational problem (4) on $\overline{T}_j^h$, $j\in E$, will also be based on the $k-th$ order Lagrange elements, after transforming the exponentially compressed polar meshes to square meshes with side length β_j using the variables

$$x'=\ln r_j,\ y'=\theta_j. \tag{23}$$

Finally, we let $G_h\equiv G_h^*\cup\left(\cup_{j\in E}\overline{T}_j^h\right)$ denote the finite element mesh formed in G. The boundary of G_h is defined as follows. Let

$$\tilde{\gamma}_j=\{(r_j,\theta_j): j\in E, 0\le r_j\le r_{j\nu_j}, \theta_j=0\},$$

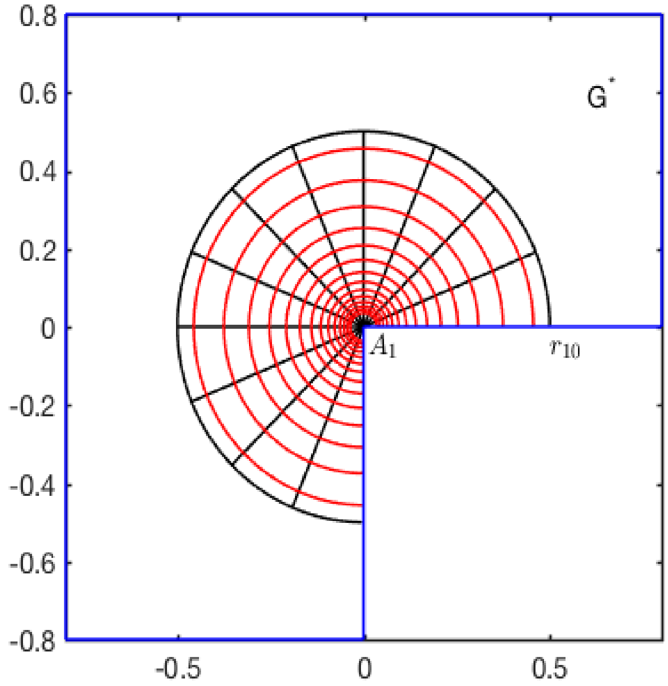

Figure 2: *Exponentially compressed polar mesh on a polygon with one singular corner.*

$$\tilde{\gamma}_{j-1} = \{(r_j, \theta_j) : j \in E, 0 \le r_j \le r_{j\nu_j}, \theta_j = \alpha_j \pi\},$$

and $\tilde{\gamma} = \cup_{j\in E}(\tilde{\gamma}_j \cup \tilde{\gamma}_{j-1})$. Then the boundary of G_h is formed as $\gamma' = (\gamma \backslash \tilde{\gamma}) \cup (\cup_{j\in E} \vartheta_{j\nu_j})$.

We denote by V_h the finite element subspace of H_E^1, and by $V_h^{\gamma'}$ the restriction of V_h to the boundary γ'. Let $u_\phi^h \in V_h^{\gamma'}$ be the interpolant of the boundary functions (2) on $\gamma\backslash\tilde{\gamma}$, and (22) on the artificial boundary $\vartheta_{j\nu_j}$, $j \in E$.

The corresponding approximation problem to the variational problem (4) is as follows: Find $u_h \in V_h$ such that $u_h|_{\gamma'} = u_\phi^h$, and

$$a(u_h, v) = (f, v) \text{ for all } v \in V_h^0, \tag{24}$$

where $V_h^0 = V_h \cap H_0^1$.

Remark 1. As the solution might only have a weak singularity in the vicinity of the corners with interior angle $\alpha_j\pi$ when $0 < \alpha_j < 1$, $j \in E$, there is no need to construct exponentially compressed polar meshes near these corners when the required accuracy of the approximate solution is $O(h)$ in the H^1-norm.

4 Error Analysis

Let $u_\phi \in H_E^1$, which clearly takes the value ϕ_j on γ_j, $j = 1, 2, ..., N$, and define ([25], p. 70)

$$H_E^1 = u_\phi + H_0^1.$$

Since the solution of problem (4) $u \in H_E^1$, we let $u_0 = u - u_\phi$, where $u_0 \in H_0^1$, and reformulate problem (4) as follows: Find $u_0 \in H_0^1$ such that

$$a(u_0, v) = (f, v) - a(u_\phi, v) \ \forall v \in H_0^1(G). \tag{25}$$

The corresponding approximation problem is: For the finite-dimensional subspace $V_h^0 \subset H_0^1$, find $u_0^h \in V_h^0$ such that

$$a(u_0^h, v) = (f, v) - a(u_\phi^h, v) \ \forall v \in V_h^0. \tag{26}$$

It can be easily verified that the conditions of the Lax-Milgram theorem are satisfied, and hence solutions to problems (25) and (26) exist and are unique ([22], [23]).

We let $\{\varphi_1, ..., \varphi_{n_e}\}$ denote the set of basis functions of the finite element space V_h^0, define the additional functions φ_i, $i = n_e + 1, ..., n_e + n_\gamma$, by extending the space V_h^0 to V_h, and select the fixed coefficients $\mathbf{u}_i$, $i = n_e + 1, ..., n_e + n_\gamma$, so that

$$u_\phi^h = \sum_{i=n_e+1}^{n_e+n_\gamma} \mathbf{u}_i \varphi_i \tag{27}$$

is the $k - th$ order $V_h^{\gamma'}$ interpolant of the boundary functions (2) on $\gamma\backslash\tilde{\gamma}$, function (22) on $\vartheta_{j\nu_j}$, $j \in E$, and has the value zero at all remaining nodes.

Accordingly, the approximate solution takes the form

$$u_h = \sum_{i=1}^{n_e} \mathbf{u}_i \varphi_i + \sum_{i=n_e+1}^{n_e+n_\gamma} \mathbf{u}_i \varphi_i,$$

where $\mathbf{u}_i$, $i = 1, ..., n_e$, are coefficients to be determined.

Everywhere below we will denote constants which are independent of h by $c, c_0, c_1, ...$, generally using the same notation for different constants for simplicity.

Theorem 1. *Let u be the solution of the variational problem (4) and u_h be the solution of the corresponding approximation problem (24). Then*

$$\|u - u_h\|_{1,G_h} \leq ch^k, \tag{28}$$

for any integer $k \geq 1$.

Proof. For the error bound of the solution on the finite element mesh G_h^*, taking (3), (17) and (27) into account, by Corollary 5 in [24], interpolation theory and Theorem 4 in [20], for any integer $k \geq 1$ we have the estimate

$$\|u - u_h\|_{1,G_h^*} \leq ch^k. \tag{29}$$

Now, we analyze the error bound of the solution on the sector T_j^h, $j \in E$. Without loss of generality, let the radius of the sector $r_{j0} = 1$.

We consider T_j^h under the mapping (23), in the $x', y'-$plane. For simplicity, we keep the same notation. From (12), (13) and (16) it follows that the solution of the boundary value problem (7), (8) in T_j^h takes the form

$$u(x', y') = O(e^{x'/\alpha_j}), \tag{30}$$

and

$$|u|_{k+1,\overline{T}_j^h} < \infty. \tag{31}$$

Let $\Pi_h u$ denote the V_h-interpolant of u, and let $\hat{u}_h \in V_h$ such that $\hat{u}_h|_{\gamma'} = u_\phi^h$. Since $\hat{u}_h \in V_h$ is arbitrary, from inequality (2.8) in [24] it follows that

$$\|u - u_h\|_{1,T_j^h} \leq c_0 \inf_{\substack{\hat{u}_h \in V_h \\ \hat{u}_h|_\gamma = u_\phi^h}} \|u - \hat{u}_h\|_{1,T_j^h}. \tag{32}$$

By the triangle inequality,

$$\|u - \hat{u}_h\|_{1,T_j^h} \leq \|u - \Pi_h u\|_{1,T_j^h} + \|\Pi_h u - \hat{u}_h\|_{1,T_j^h}. \tag{33}$$

Now, from interpolation theory, (31) and (20)

$$\|u - \Pi_h u\|_{1,T_j^h} \leq c_1 \beta^k |u|_{k+1,T_j^h} \leq c_3 h^k. \tag{34}$$

We may choose $\hat{u}_h$ so that it has the same value at all interior nodes as the interpolant $\Pi_h u$. Then $(\Pi_h u - \hat{u}_h) = 0$ in $\overline{T}_j^h$ except for the layer of elements adjacent to the side l_j, with thickness $O(\beta_j)$, since $\hat{u}_h = \Pi_h \tilde{\phi}_j^*$ on the side l_j of T_j^h, where $\tilde{\phi}_j^*(x', y')$ is the Lagrange polynomial (22) under the transformation (23). The side l_j denotes the arc $\vartheta_{j\nu_j}$ defined in Section 3, under the mapping (23), which is the line $l_j = (-\nu_j \beta_j, y')$, $0 \leq y' \leq \alpha_j \pi$.

By the triangle inequality, the inverse trace theorem [26] and an inverse inequality [23], we have

$$\|\hat{u}_h - \Pi_h u\|_{1,T_j^h} \leq c_2 \beta_j^{-(1/2)} \|\Pi_h \tilde{\phi}_j^* - u\|_{\infty,l_j} + \|\Pi_h u - u\|_{1,T_j^h}. \tag{35}$$

Since $\tilde{\phi}_j^*$ is a linear polynomial, $\Pi_h \tilde{\phi}_j^* = \tilde{\phi}_j^*$. It is easy to show that

$$| \tilde{\phi}_j^*(y') - u(-\nu_j \beta_j, y') | \leq c_3 \max_{0 \leq \xi \leq \alpha_j \pi} \left| \frac{\partial^2 u}{\partial y'^2}(-\nu_j \beta_j, \xi) \right|. \tag{36}$$

Hence by (30), (36) and the norm

$$\|f\|_{\infty,S} = ess\sup_{x\in S}|f(x)|,$$

it follows that

$$\|\tilde{\phi}_j^* - u\|_{\infty,l_j} \le c_4 e^{-\nu_j\beta_j/\alpha_j}. \tag{37}$$

By virtue of (21), when $\min\{1, 1/\alpha_j\} = 1/\alpha_j$,

$$\begin{aligned} e^{-\nu_j\beta_j/\alpha_j} &\approx \exp\left(-\frac{\beta_j}{\alpha_j}\left[\frac{k+1/2}{\beta_j}\frac{\ln h^{-1}}{1/\alpha_j}\right]\right) \\ &\approx \exp\left(\ln h^{k+1/2}\right) = h^{k+1/2}, \end{aligned}$$

and when $\min\{1, 1/\alpha_j\} = 1$,

$$\begin{aligned} e^{-\nu_j\beta_j/\alpha_j} &\approx \exp\left(-\frac{\beta_j}{\alpha_j}\left[\frac{k+1/2}{\beta_j}\ln h^{-1}\right]\right) \\ &\approx \exp\left(\ln h^{(k+1/2)/\alpha_j}\right) = h^{(k+1/2)/\alpha_j} \le h^{k+1/2} \end{aligned}$$

as $0 < h < 1$ and $1/\alpha_j > 1$.

Hence it follows from (37) that

$$\|\tilde{\phi}_j^* - u\|_{\infty,l_j} \le c_5 h^{k+1/2}. \tag{38}$$

Combining (32)-(35), (37) and (38) we have

$$\|u - u_h\|_{1,T_j^h} \le c_6 h^k, \;\; k \ge 1 \text{ an integer}. \tag{39}$$

Since the number of sectors T_j^h, $j \in E$ is finite, by (39),

$$\|u - u_h\|_{1,\cup_j T_j^h} \le c_7 h^k. \tag{40}$$

Finally, taking into account that the finite-element mesh G_h is conforming, by (29) and (40) inequality (28) follows. □

5 Numerical Example

To test the effectiveness of the method, a numerical example is computed in an L-shaped domain (see Figure 2), where the exact solution has a corner singularity at the vertex A_1 with an interior angle $\alpha_1\pi = 3\pi/2$. For the implementation of the method, linear and bilinear Lagrange elements were used so that an accuracy of $O(h^2)$ is obtained in the L^2 relative error norm, where h is defined as in Section 3. The calculations were carried out in Fortran 90 with double precision. The radius r_{10} of the sector T_1 is taken as 1 for all mesh sizes $h = 2^{-m}, m = 3, 4, 5, 6, 7$.

Example 1. Let G be the L-shaped domain defined as

$$G = \{(x, y) : -2 < x < 2, -2 < y < 2\} \backslash G_1,$$

where $G_1 = \{(x, y) : 0 \le x \le 2, -2 \le y \le 0\}$, and let γ be the boundary of G. We consider the following problem.

$$-\Delta u + u = f \text{ in } G, \tag{41}$$

$$u = v(r, \theta) \text{ on } \gamma, \tag{42}$$

where $v(r,\theta) = I_{2/3}(r)\sin\left(\frac{2\theta}{3}\right) + r^3\cos(\theta)$ is the exact solution of this problem and $f(r,\theta) = (r^3 - 8r)\cos(\theta)$. The expected solution to problem (41), (42), cannot be computed with arbitrary accuracy since it requires the summation of an infinite Bessel series. We present the error and the convergence rate, for completeness, defined as

$$\frac{\|u - u_{2^{-m}}\|_{0,G_h}}{\|u\|_{0,G_h}} \text{ and } \frac{\|u - u_{2^{-m}}\|_{0,G_h}}{\|u - u_{2^{-(m+1)}}\|_{0,G_h}},$$

respectively in Table 1, where $u_{2^{-m}}$ denotes the numerical solution obtained on the finite-element mesh with $h = 2^{-m}, m = 3, 4, 5, 6, 7$. A partial sum of the Bessel series was used for the boundary functions and the exact solution, with accuracy at computer precision. Since this is not a very accurate measure, we also present the convergence rate obtained by comparing the numerical solution attained in T_1^h on successive grids, where the convergence rate on the grid with $h = 2^{-m}$ is defined as

$$\frac{\|u_{2^{-(m+1)}} - u_{2^{-m}}\|_{0,T_1^h}}{\|u_{2^{-(m+1)}} - u_{2^{-(m+2)}}\|_{0,T_1^h}}.$$

The $O(h^2)$ accuracy corresponds to 2^2 for convergence rate. The results are presented in Table 2. The value of ν_1 is chosen such that the number of element nodes are consistent on each successive grid. As demonstrated in Table 1, smaller values of ν_1 would still be sufficient for convergence.

$(2^{-m}, \nu_1)$	L^2 - Relative Error	L^2 - Convergence Rate
(3,100)	2.0880E-003	
(4,200)	4.5744E-004	4.5645
(5,350)	1.2140E-004	3.7678
(6,600)	3.1391E-005	3.8674
(7,800)	7.8252E-006	4.0115

Table 1: The relative error and convergence rate of problem (41), (42) in the L^2 Norm.

$(2^{-m}, \nu_1)$	Convergence Rate
(3,100)	
(4,200)	
(5,400)	4.05969
(6,800)	3.97003
(7,1600)	4.01633

Table 2: The convergence rate of problem (41), (42) on successive grids.

6 Concluding Remarks

A highly-accurate finite element method has been developed and justified for the approximate solution of the generalized Helmholtz equation with Dirichlet boundary conditions on polygons. The method is based on the $k-th$ order Lagrange elements for the finite element discretization on triangular and curved meshes in the part of the domain away from corners, and on exponentially refined polar meshes near singular corners. For the error bound between the exact and the approximate solution, an accuracy of $O(h^k)$, $k \geq 1$ an integer, is obtained in the H^1-norm.

The implementation of the method is straight forward since the polar meshes transform to square meshes in Log-Polar coordinates. Hence the derivation of a new algorithm or the design of a mesh specific to a corner is not required.

A numerical example has been solved in an L-shaped domain and the results are consistent with the theoretical results obtained. For the implementation of the numerical example, the approximate solution has been based on linear Lagrange polynomials. Nevertheless, when the order of the used basis polynomials is increased, there is no need to compress the mesh more aggressively to obtain higher accuracy. The only difference in setting up the compressed mesh will be in the value of ν_j given in (21). By definition, the value of this parameter depends on the order of the applied Lagrange polynomials.

The proposed method can also be used for the solution of the Laplace and Poisson's equations with Dirichlet boundary conditions.

Another application of the method is to the case when the constant in equation (1), $a_0 < 0$. In the vicinity of the corners, the analytical solution of this problem will have the same regularity as (9). Furthermore, the proposed method can be applied in domains whose 'non-singular' part has a curved boundary.

Finally, the method can be employed for dealing with the corner singularities of general nonlinear parabolic partial differential equations with semi-implicit time discretization.

The use of the presented method for the solution of the generalized Helmholtz equation with Neumann, Robin or mixed boundary conditions is not trivial. However it will be possible to extend the method by taking into account the change that will be required in the boundary condition (22), which is applied on the artificial boundary of the grid. We note that this will also reflect on the choice of ν_j given in (21).

Acknowledgements

E. Celiker's work is supported by the EU Scholarship Programme for the Turkish Cypriot Community 2017/18.

References

[1] Babuška, I., and Oh, H. S. (1990) *The p-version of the finite element method for domains with corners and for infinite domains.* Numerical Methods for Partial Differential Equations, 6(4), 371-392. Chicago.

[2] Thatcher, R. W. (1976) *The use of infinite grid refinements at singularities in the solution of Laplace's equation.* Numerische Mathematik, 25(2), 163-178.

[3] Burda, P., Novotný, J., Šístek, J. (2005) *Precise FEM solution of a corner singularity using an adjusted mesh.* International journal for numerical methods in fluids, 47(10-11), 1285-1292.

[4] Fix, G. (1969) *Higher-order rayleigh-ritz approximations.* Journal of Mathematics and Mechanics, 18(7), 645-657.

[5] Wait, R., and Mitchell, A. R. (1971) *Corner singularities in elliptic problems by finite element methods.* Journal of Computational Physics, 8(1), 45-52.

[6] Li, Z. C. (1986) *A nonconforming combined method for solving Laplace's boundary value problems with singularities.* Numerische Mathematik, 49(5), 475-497.

[7] Dosiyev, A. A. (2004) *The high accurate block-grid method for solving Laplace's boundary value problem with singularities.* SIAM Journal on Numerical Analysis, 42(1), 153-178.

[8] Wu, X., and Han, H. (1997) *A finite-element method for Laplace-and Helmholtz-type boundary value problems with singularities.* SIAM Journal on Numerical Analysis, 34(3), 1037-1050.

[9] Xenophontos, C., Elliotis, M., and Georgiou, G. (2006) *A singular function boundary integral method for Laplacian problems with boundary singularities.* SIAM Journal on Scientific Computing, 28(2), 517-532.

[10] Volkov, E. A. (1994) *Block Method for Solving the Laplace Equation and Constructing Conformal Mappings.*

[11] Magura, S., Petropavlovsky, S., Tsynkov, S., and Turkel, E. (2017) *High-order numerical solution of the Helmholtz equation for domains with reentrant corners.* Applied Numerical Mathematics, 118, 87-116.

[12] Li, Z. C., and Lu, T. T. (2000) *Singularities and treatments of elliptic boundary value problems.* Mathematical and Computer Modelling, 31(8-9), 97-145.

[13] Apel, T., and Milde, F. (1996)*Comparison of several mesh refinement strategies near edges.* International Journal for Numerical Methods in Biomedical Engineering, 12(7), 373-381.

[14] Oganesyan, L. A., and Rukhovets, L. A. (1979) *Variational-difference methods for the solution of elliptic equations.* Izd. Akad. Nauk Armyanskoi SSR, Jerevan.

[15] Huang, C., Wu, Z., and Nevels, R. D. (1993) *Edge diffraction in the vicinity of the tip of a composite wedge.* IEEE transactions on geoscience and remote sensing, 31(5), 1044-1050.

[16] Volkov, E. A. (1976) *On the method of composite meshes for Laplace's equation on polygons.* Trudy Mat. Inst. Steklov. V.140. P.68-102 (In Russian).

[17] Dosiyev, A. A. (2002) *A fourth-order accurate composite grid method for solving Laplace's boundary value problems with singularities.* Zh. Vychisl. Mat. Mat. Fiz., 42(6), 867-884.

[18] Volkov, E. A., and Dosiyev, A. A. (2007) *A high accurate composite grid method for solving Laplace's boundary value problems with singularities.* Russian Journal of Numerical Analysis and Mathematical Modelling, 22(3), 291-307.

[19] Zlámal, M. (1973) *Curved elements in the finite element method I.* SIAM Journal on Numerical Analysis, 10(1), 229-240.

[20] Zláman, M. (1974) *Curved elements in the finite element method II.* SIAM Journal on Numerical Analysis, 11(2), 347-362.

[21] Zlámal, M. (1973) *The finite element method in domains with curved boundaries.* International Journal for Numerical Methods in Engineering, 5(3), 367-373.

[22] Ciarlet, P. G. (1978) *The finite element method for elliptic problems.* Amsterdam, New York, Oxford: North Holland.

[23] Brenner, S. and Scott, R. (2007) *The mathematical theory of finite element methods.* Vol. 15. Springer Science and Business Media.

[24] Fix, G. J., Gunzburger, M. D., and Peterson, J. S. (1983) *On finite element approximations of problems having inhomogeneous essential boundary conditions.* Computers and mathematics with applications, 9(5), 687-700. Chicago.

[25] Strang, G., and Fix, G. J. (1973) *An analysis of the finite element method (Vol. 212).* Englewood Cliffs, NJ: Prentice-hall.

[26] Hsiao, G. C., and Wendland, W. L. (2008) *Boundary integral equations.* Springer Berlin Heidelberg.